Geophys. J. Int. (2007) doi: 10.1111/j.1365-246X.2006.03298.x

Anomalous seismicity preceding the 1999 Izmit event, NW Turkey

Ali O. Oncel[1] and Tom Wilson[2]

[1] *Earth Sciences Department, King-Fahd University of Petroleum & Minerals, Saudi Arabia. E-mail: oncel@hotmail.com*
[2] *Department of Geology and Geography, West Virginia University, United Sates*

Accepted 2006 November 14. Received 2006 November 14; in original form 2005 March 25

SUMMARY

The 1999 Izmit earthquake (1999 August 17, $M_w = 7.4$) was one of the largest earthquakes to occur in northwestern Turkey during the past 100 yr. This earthquake occurred along the Izmit–Sapanca fault within the Northern Anatolian Fault Zone. Variations in the generalized fractal dimensions (D_q) of clustering in time and space, the Gutenberg–Richter *b*-value, and earthquake frequency (N) are evaluated in detail over an 8.5 yr time period preceding the Izmit event. Spatial and temporal comparisons of the variations in these parameters reveal anomalous intermediate term behaviour over shorter timescales than previously observed. Significant correlation is observed between changes in *b*-value with the spatial and temporal fractal dimension of epicentre distribution. These correlations oscillate back and forth over 2–3 yr time intervals and suggest occurrence of significant instability in the nature of intermediate-term deformation along the fault zone. Seismotectonic behaviour immediately preceding the Izmit event is represented by a significant rise in *b*-value to a maximum of 2.26 accompanied by relatively small increases in *D*. The rapid rise of *b* is associated with an increased frequency of low magnitude seismicity. Although *D* (spatial and temporal) increase slightly in the 2–3 yr period preceding rupture, they remain less than 1 indicating that seismicity remains clustered prior to rupture. In areas where earthquake frequency or station density do not permit resolution of short-term variations of *fractal scaling parameters* within a few months of main rupture, an accelerated period of low-magnitude seismicity (high *b*-value) concentrated along a fault zone ($D < 1$) may suggest heightened probability of a forthcoming large event.

Key words: Geodetic moment, GPS strain, Izmit, multifractal, seismicity, seismotectonic.

1 INTRODUCTION

Precursory anomalies preceding a large magnitude earthquake can be divided into long-term (10–30 yr), intermediate (1 month to 10 yr) and short-term (hours to weeks) behaviour (Scholz 2002). Precursory variations in the fractal properties of seismicity distribution may serve as an intermediate warning of future main shocks (e.g. Main 1996; Henderson *et al.* 1994; Nakaya & Hashimoto 2002; Scholz 2002). Henderson & Main (1992) and Henderson & Main (1992) examine temporal changes in *b*-value, D_S (spatial fractal dimension) and the correlation between them prior to rupture in laboratory triaxial stress tests. Their laboratory tests reveal a gradual rise in *b* followed by a gradual fall. Prior to the California Coalinga earthquake in 1983; *b*-value rose gradually for more than a year to ~2.25 and then fell abruptly over a 2–3 month period to about 1.8 at the time of rupture (Main *et al.* 1989). Oscillations in *b*-value from high to low and back again occurred at 4 and 6 yr intervals in the 10 yr preceding the Coalinga event. The intermediate term increases in *b*-value were followed by a sharp, short-term, decrease prior to the major event. Oscillations in the fractal pattern of seismicity were also observed preceding Western Tottori earthquake ($M = 7.3$) (see fig. 4 of Nakaya & Hashimoto 2002). Cyclical variations included a decrease in fractal dimension preceding a period during which the fractal dimension rose to a maximum at the time of the main shock.

Temporal variations of *b*-value were used by Henderson & Main (1992) to distinguish between positive and negative feedback fault interactions. Negative feedback processes are associated with widely distributed fault systems. Fault growth in response to applied stress reduces the stress intensity in the vicinity of the fault and further growth of the fault. There is a negative feedback between increased fault length and stress intensity. Sets of widely distributed, non-interacting, faults deform gradually over time. Individual faults do not accelerate to failure because of the negative feedback between fault extension and local stress intensity: fault tip failure and extension automatically reduce stress concentration and further fault propagation. If, on the other hand, the fault density increases to the point where stress intensity at the tip of the fault is influenced by neighbouring faults, then a runaway positive feedback process can develop such that stress intensity increases with fault length. Development of a positive feedback response leads to rapid failure.

The negative feedback process is associated with distributed fault systems. Such systems have D_0 (fractal dimension determined from box counting) greater than 1. Fault rupture is generally restricted to faults of relatively small length and surface area so that *b* tends to

be relatively large: D_0 and b increase together leading to a positive correlation (see Henderson & Main 1992). Transition to a positive feedback process is defined by clustering of larger magnitude seismicity and also yields a positive correlation between b and D_0. As faults begin to coalesce (i.e. become clustered), earthquake magnitude increases with increasing fault length and area: both D_0 and b decrease together.

In this study, we focus on the evaluation of relationships between b and D_q along the Izmit–Sapanca fault in the 8.5 yr period prior to the 1999 Izmit event. The multifractal dimension D_q was evaluated in time and space; q varied from 2 to 15. Analysis of temporal variability in the spatial correlation dimension (D_2) along major subdivisions of the central and western parts of the NAFZ documented in earlier work (Öncel *et al.* 1995; Oncel *et al.* 1996; Oncel & Wilson 2002) revealed significant changes through time in seismic clustering (D_2). Prior analysis of changes in spatial D_2 (fractal dimension of seismicity distribution) along the NAFZ have also been correlated to changes in b-value (Öncel *et al.* 1995; Oncel *et al.* 1996; Oncel & Wilson 2002). Some of these correlations may be due to changes in station density (Öncel *et al.* 1995), while others reflect changes of tectonic interaction (Oncel *et al.* 1996). Recent evaluation of these relationships reveals significant change in the correlation between D and b preceding the Izmit event (Oncel & Wilson 2002, 2004).

The Izmit event is the first Anatolian event for which the preceding seismicity has been continuously monitored by a single modern seismological network (MARNET). The Izmit earthquake (M_w = 7.4) is associated with rupture of the Izmit–Sapanca fault which is the northern strand of the NAFZ extending from Adapazari at about 31°E through the Marmara Sea to 29°E (Fig. 1). Earthquake distribution (Fig. 1) suggests that this fault coincides with a potential seismic gap across the Lake Sapanca area (Toksoz *et al.* 1979) or asperity (Oncel & Wyss 2000a,b). In this paper, we characterize seismicity using multifractal evaluation of seismicity distribution (D_q) in time and space, the Gutenberg–Richter b-value and the event rate (N). To our knowledge, this study is the first to evaluate and compare multifractal behaviour of precursory seismicity in both time and space. Comparisons of these parameters are made using seismicity recorded from 1991 January 5 to 1999 June 6 (ending approximately 2 months prior to the Izmit event). Changes in these parameters and their interrelationship through time will be used to draw inferences about potential variations in underlying crustal stress leading to final rupture of the Izmit–Sapanca fault zone.

2 DATA

2.1 GPS derived strain

The geodetic moment rate (M_{geodetic}) is estimated from the maximum strain rate ($\dot{\varepsilon}_{\max}$) using Kostrov's (1974) formula:

$$M_{\text{geodetic}} = 2\mu A H_s \dot{\varepsilon}_{\max}. \quad (1)$$

In this case, $\dot{\varepsilon}_{\max}$ – the larger of the absolute values of λ_1 or λ_2 – is determined using the methodology of Ward (1994), where λ_1 or λ_2 is the principal component of absolute strain rate presented by Kahle *et al.* (2000) for the 1988 to 1998 time period. μ, is the shear rigidity (assumed to be 3×10^{10} N m^{-2}), H_s is the thickness of the seismogenic zone, and A is the surface area over which strain release is distributed. In this study, we use $A = L^2$ where L is the fault length associated with an $M_w = 7.4$ earthquake. H_s is the crustal thickness. We preferred the 12.5 km value for H_s, which

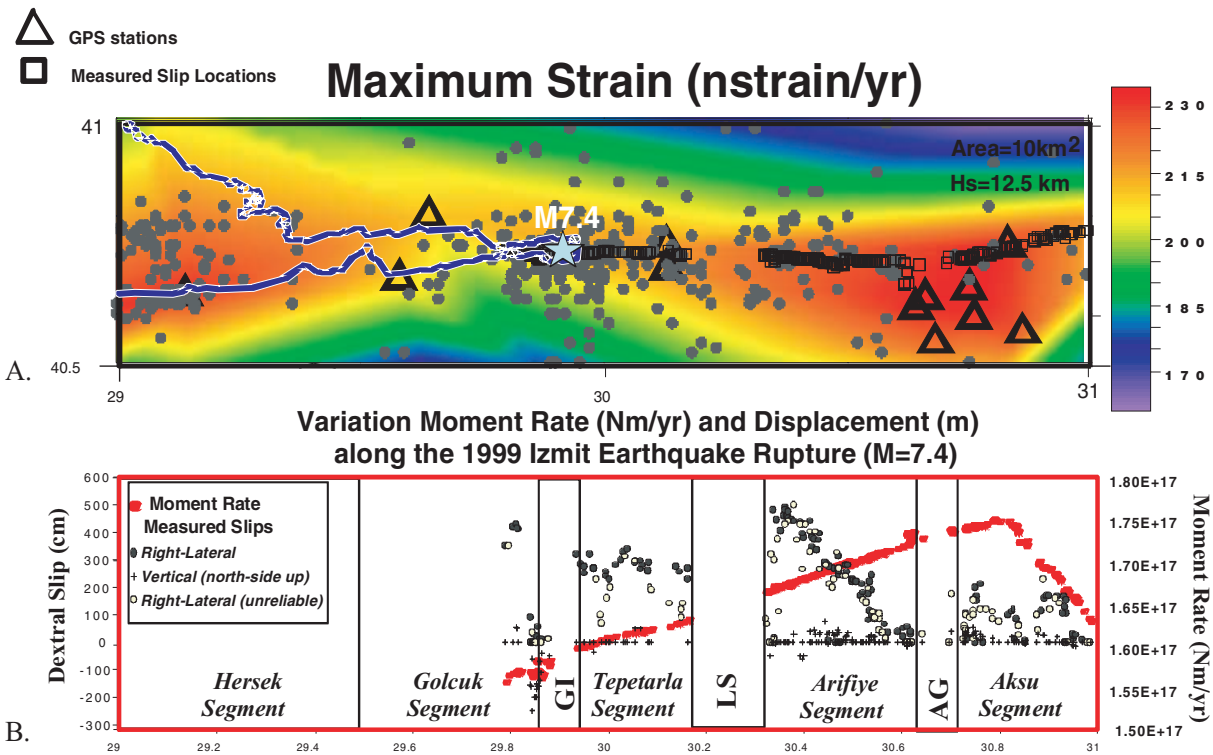

Figure 1. (a) Maximum GPS strain (1988–1998) is shown in color, along with epicentre locations and fault displacement measurement points. (b) Dextral slip and moment rate associated with the Izmit event are plotted along the length of the Izmit–Sapanca fault (Awata *et al.* 2003). Fault segments and seismic gaps are labelled for reference. LS: Lake of Sapanca, GI: Gulf of Izmit, AG: Akyazi Gap. Hs = Thickness of the seismogenic zone.

represents an average crustal thickness in the Marmara Sea region (Ambraseys 2002). Maximum strain distribution through the region (Fig. 1) was determined by triangulation with linear interpolation. Measured slip rates presented by Awata *et al.* (2003) are compared to geodetic moment rate which was calculated in this paper from eq. (1). The map provides a view of pre-earthquake strain associated in part with the time interval evaluated in this study. Maximum strain is narrowly distributed along the central part of the rupture zone (Golcuk and Tepetarla segments) and is distributed across a wider band in areas to the east and west (Fig. 1a).

Geodetic moment rate (1981–1998) rises linearly, west-to-east, along the Izmit–Sapanca fault from Golcuk into the Aksu segments. Within the Aksu segment moment rate drops abruptly, east of longitude 30.8° (Fig. 1). The pattern of measured slip (see fig. 1, from Awata *et al.* 2003) is non-uniform. The characteristics of slip along the Izmit–Sapanca fault can be described as approximately constant along the Tepatarla segment at about 300 cm (dextral), as dropping from nearly 500 cm to 0 (west to east) along the Arifiye segment, and as approximately constant at 100 cm across the Aksu segment (Fig. 1). Lake Sapanca and the Akyazi Gap mark the locations of abrupt changes in net slip along the Izmit–Sapanca fault.

2.2 Seismicity data

In recent years, a large number of seismographs have been added to the seismological networks (MARNET and IZINET) that monitor the Marmara (Evans *et al.* 1982, 1985; Ucer *et al.* 1985) and Izmit regions (Ito *et al.* 2002), respectively. Errors in epicentre location and depth are estimated to be 1.8 km with a standard error of ±1.1 km and 3.4 km with a standard error of ±3.6 km, respectively (Akihiko Ito, 2004, personal communication). Given the larger errors in depth, the estimates of spatial fractal dimension (D_S) were derived from the epicentre distribution rather than the hypocentre distribution. Errors in spatial location have no effect on the estimates of the temporal fractal dimension (D_T). The increased station density yielded considerable improvement in the quality of data recorded by these networks. The MARNET and IZINET networks have contributed significantly to a better understanding of crustal heterogeneity and fault activity in this area of northwestern Turkey (Ito *et al.* 2002; Ucer *et al.* 1985). Several major cities including Istanbul are located in this high seismic risk region. Recent improvements to the networks provide increased sensitivity that is critical to the accurate measurement of changes in the frequency, magnitude, and distribution of earthquakes in the region (Öncel *et al.* 1995; Oncel & Wyss 2000a,b).

The geographic extent of the earthquake slip area lies between longitudes of 29°–31°E and latitudes of 40.5°–41°N (see Fig. 1). Although data evaluated in this study span the 1991 January–1999 June time interval, the requirement that individual analysis windows contain at least 100 events resulted in average times that extended from 1991.95 to 1998.24. Analysis of declustered seismicity compiled from the MARNET catalogue in the region conducted by Öncel & Alptekin (1999) reveals a magnitude shift of 0.3 and change in the completeness magnitude (M_c) in 1990 from 2.6 (1981–1989) to 2.9 (1990–1998) after shift correction (see also Oncel & Wyss 2000a). Analysis of data restricted to this time interval avoids the artificial influences on seismicity rate associated with changes in the seismograph array that occurred prior to 1990.

Temporal variations in threshold magnitude were examined during the analysis period following the suggestions of Wiemer & Wyss (2000). The analysis was conducted using ZMAP software (Wiemer 2001). We subdivided the data into 100 event windows covering a 20 × 20 km area. The time-shift (Fig. 2a) was variable and corresponded to the time during which 10 additional events were observed. The spatial analysis of threshold magnitude (Fig. 2b) was also conducted for 100 event windows. Consecutive spatial windows were shifted on average by 5 km steps. Variations in M_c from 1991 to June of 1999 (Fig. 2a) reveal that the $M_c = 2.9$ used in this study is a conservative threshold. Temporal variations in completeness magnitude spanning the period of analysis range between 2.5 and 2.8. The spatial distribution of M_c (Fig. 2b) reveals a systematic increase in M_c from west to east through the study area. The constraints imposed by the 8.5 yr time window and M_c of 2.9 limited data used in the analysis to approximately 400 events. We use a fault-specific area restricted to the region surrounding the Izmit event and shorter time window than that used in previous studies (Oncel & Wyss 2000, 2001). The number of events recorded from 1991 to 1999 was 1338 for $M > 2$. However, many of these events were excluded due to our use of a completeness magnitude of $M = 2.9$ which left about 400 events in the current study. Variations in the cumulative number of events increase linearly through the period of analysis (Fig. 3).

The shorter period of analysis (1991–1999.5) in the present study combined with use of the raw catalogue leads to differences in the results obtained by Oncel & Wyss (2000) and those obtained in the present study. The entire record of seismic behaviour provided by the raw catalogue may yield valuable insights into anomalous seismic behaviour preceding the Izmit event. Other approaches (e.g. Oncel & Wyss 2000; Oncel *et al.* 2001) prefer to use the declustered catalogue to characterize the phenomena of asperity and seismotectonic zonation. In this study, our aim is to examine seismicity patterns and their interrelationship to various seismicity parameters. The magnitude used in this study is the duration magnitude 'M_D'. M_D is the most common magnitude reported by the Turkish seismic networks operated by Kandilli Earthquake Research Institute (KOERI). M_D is believed to be a more reliable measure of background seismicity because of saturation problems associated with other magnitude measures (e.g. M_L and M_B) (Castellaro *et al.* 2006).

We investigate the detailed record for evidence of anomalous seismicity preceding larger events. Seismicity included in the analysis consisted of approximately 400 events of $M_D > 2.9$ for the years between 1991 (1991 January 5) and 1999.5 (1999 June 6). The threshold magnitude of $M_D = 2.9$ limits the influence of site effects such as local swarm activity on estimated seismicity variables.

Temporal changes in *b*-value and the generalized fractal dimension (D_q) were estimated for sliding windows whose duration was varied to contain 100 consecutive events. Consecutive windows were advanced through time by 10 event increments to provide a time-series representation for each of these seismotectonic variables.

3 METHOD

3.1 *b*-value and event rate (N)

The Gutenberg & Richter (1954) relation:

$$\mathrm{Log}N = a - bM \tag{2}$$

implies a fractal relation between earthquake frequency and magnitude. Fractal behaviour extends to the distribution of radiated energy, seismic moment, and fault length through their interrelationship to magnitude. The *b*-value is widely used to describe the size scaling properties of seismicity. N is seismic event rate and the log(N) is linearly related to earthquake magnitude (M). The intercept (a)

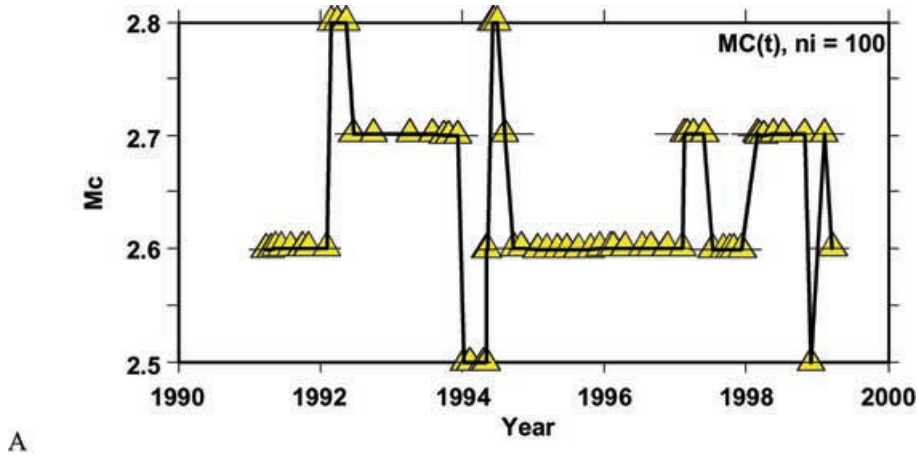

A

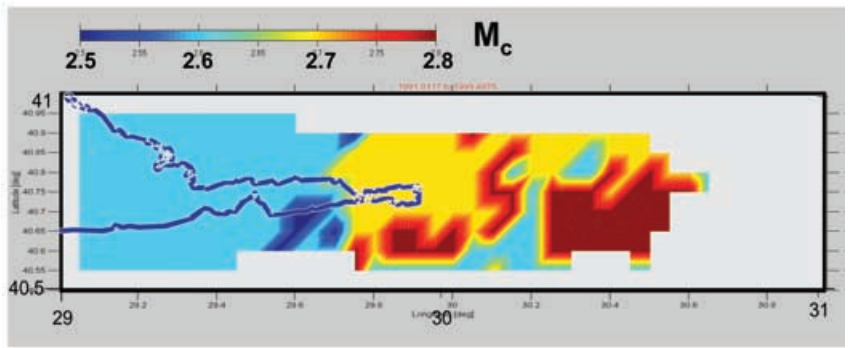

B.

Figure 2. (a) Time-variation of threshold magnitude for 100 event windows with 10 event shifts. (b) Spatial variations in threshold magnitude are mapped throughout the area. Threshold magnitude was calculated on a grid of points spaced at 0.005° intervals. Blank areas in the map are associated with nodes for which 50 or more events were not present within a 5 km radius of the point.

provides a measure of background seismicity. Shaw *et al.* (1992) suggest that variations in a may also have predictive value. The slope (b-value) defines the change in occurrence rate with magnitude. As noted, analysis was restricted to events having magnitude $\geq$2.9.

The event rate (N) for each 100-event time window is

$$N = n/T = 10^a, \tag{3}$$

where $n = 100$, T is the duration of the 100 event time window, and a is the intercept.

The b-value was estimated using the maximum likelihood method (Aki 1965)

$$b = 2.303/(M_{\text{mean}} - M_{\text{min}} + 0.05), \tag{4}$$

where M_{mean} is the mean magnitude of events with $M > M_{\text{min}}$, and M_{min} (2.9) is the minimum magnitude of completeness in the earthquake catalogue. The maximum likelihood method is considered to provide a least biased estimate of b-value. Local scale estimates of b range from 1.5 to 2.26 in the present study and are larger than the estimates of $0.5 < b < 1.6$ obtained from events of $M > 4.5$ reported in previous analysis of seismicity in this region (Öncel *et al.* 1995). The value 0.05 in eq. (4) is a correction constant that compensates for round off errors. The 95 per cent confidence limits on the estimates of b are $\pm 1.966/\sqrt{n}$, where n is the number of earthquakes used to make the estimate. This yields 95 per cent confidence limits of 0.16 $\pm$ 0.1–0.2 for sliding windows of $n = 100$ earthquakes in this study. The reference Frequency-Magnitude plot (FMP) for the entire data set (Fig. 4) includes both cumulative and discrete values. The threshold magnitude of 2.9 is clearly indicated. The b-value for the entire data set is 1.87 with 95 per cent confidence limits of $\pm$0.09.

3.2 Generalized fractal dimension

Following (Grassberger & Procaccia 1983; Smalley *et al.* 1987; Godano & Caruso 1995; Lei & Kusunose 1999; Sunmonu *et al.* 2001; Oncel & Wilson 2004, 2006) the generalized multifractal dimension, $D_{\text{q,}}$, for epicentre distribution is defined as follows:

$$D_q = \frac{1}{(q-1)} \lim_{r \to 0} \frac{\log \sum C(r)_i^q}{\log r}, \tag{5}$$

where q, in this study, is varied from 2 to 15, and $C(r)$ is the correlation integral

$$C_q(r) = \frac{1}{N} \left[\sum_{i=1}^{N} \left(\frac{N_i(R \leq r)}{N-1} \right)^{q-1} \right]^{1/(q-1)}. \tag{6}$$

N is the number of points within a distance r of point j (Smalley *et al.* 1987; Shah & Labuz 1995; Sunmonu *et al.* 2001) and R is varied from 0 to r. $C_q(r)$ gives the average fraction of epicentres within a radius r (Baker & Gollub 1990). Eqs (4) and (5) specify the spatial characteristics of the epicentre distribution. Temporal

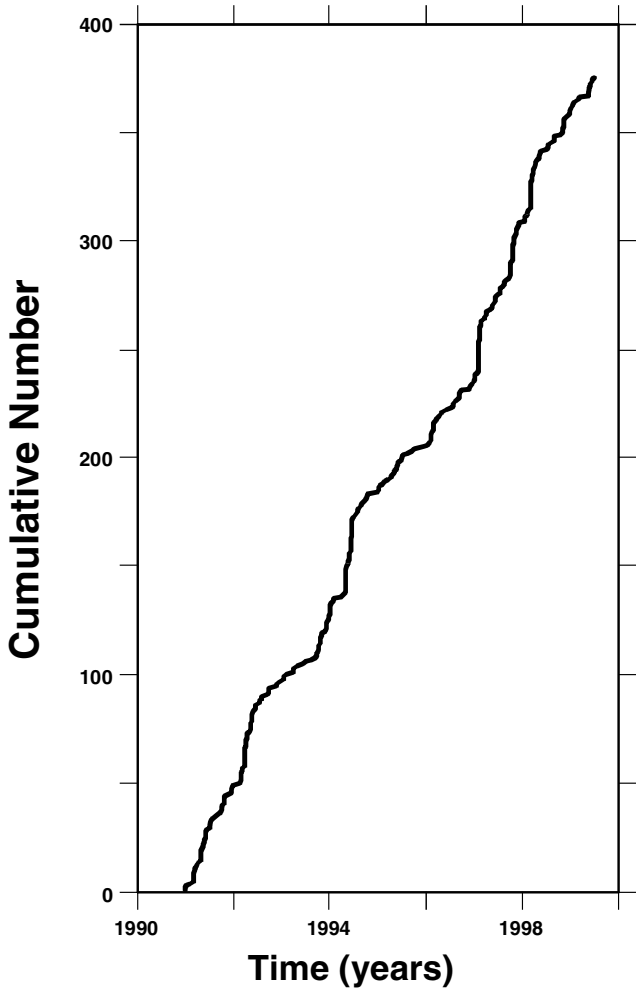

Figure 3. Cumulative number of events with $M_C \geq 2.9$ plotted through the period of time examined in this study.

variability can be estimated in a similar manner:

$$C_q(t) = \frac{1}{N}\left[\sum_{i=1}^{N}\left(\frac{N_i(T \leq t)}{N-1}\right)^{q-1}\right]^{1/(q-1)}, \quad (7)$$

where $C_q(t)$ represents the average fraction of epicentres that fall within a time window of size t. In eq. (6) we replace r with t. The multifractal parameter q was varied from 2 to 15. Multifractal dimensions D_q are estimated from the slope of the linear region of the log (C_q) versus log (r) plot in space and the slope of the linear region of the log (C_q) versus log (t) plot in time. Linearity in the relationship between log (C_q) and log (r) [or log (t)] implies a power law or fractal relationship between C_q and r [or t]. In this expression, C_q (r or t) is the number of event pairs occurring in the space range $R < r$ or in the time range $T < t$. The linear range in the log (C_q) versus log (r) or log (t) plots is specified by r_{min} and r_{max} in space, and t_{min} and t_{max} in time. Edge effects associated with saturation (at small r or t) and depopulation (at large r or t) are avoided.

We computed D_q (S and T) over a fixed range of distances and times corresponding to 7–60 km and 0.04–1.51 yr, respectively. Examples of log (C) versus log (r) plots (Figs 5a and b) immediately preceding the Izmit event reveals linear behaviour over a limited range of r and t. Note that multifractal dimensions decrease with increasing q and that D_T is less than D_S for all values of q (Fig. 5c).

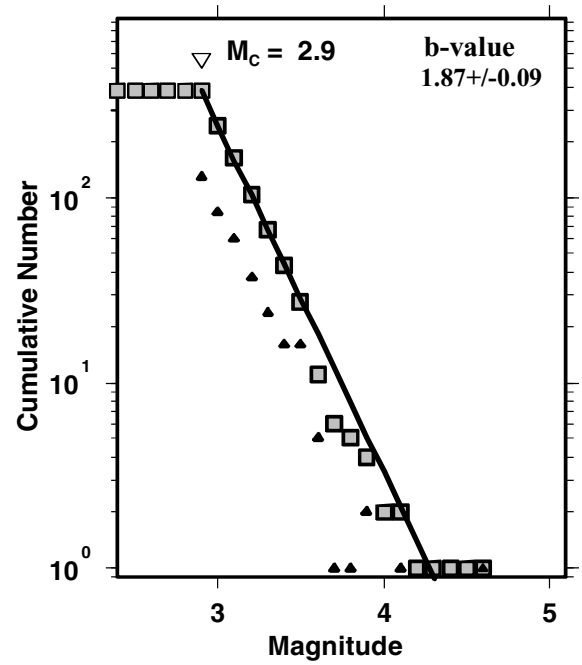

Figure 4. This frequency magnitude plot shows cumulative (squares) and discrete (triangles) numbers of events for the entire data set used in this study. The threshold magnitude associated with completeness is 2.9. The average b-value is 1.8.

The variation of D with q arises from heterogeneity in multifractal patterns of clustering in time and space. The mean standard error for $D_S(q = 2)$ is ± 0.03 (with range from 0.01 to 0.05); for $q = 15$, the standard error is ± 0.02 (with range from 0.01 to 0.05). Mean standard errors for time fractal dimensions (D_T) are ± 0.02 (0.02–0.04) for $q = 2$, and ± 0.04 (0.02–0.08) for $q = 15$.

4 OBSERVATIONS AND RELATIONSHIPS

4.1 *b*-value, magnitude and event rate

In the 7 yr interval preceding the Izmit event, the b-value fluctuated from a high of 2.1 in 1992.5 to a low of 1.6 in 1995 and then rose to an even higher value of 2.25 in early 1998 (see Figs 6a and 7). Changes in mean magnitude through this same time period (Fig. 3a) correlate inversely with b-value as expected from eq. (3).

The relationship of event rate to changes of b-value also varied through time (see Figs 6 and 7). From 1992.13 to 1993.4 (average times) log (N) is negatively correlated to b (-0.62), while from 1995.4 to 1998.4 the correlation becomes positive ($r = 0.85$) (see Fig. 7). Log (N) increases to a maximum in 1997.7 and then decreases preceding the Izmit event. During the entire 8.5 yr period of analysis, earthquake frequency remained relatively constant until mid-1996 when it began to increase steadily. A slight drop in frequency occurred 1.5 yr prior to the Izmit event.

4.1.1 Interrelationships between temporal and spatial fractal dimensions

Spatial variations of D_2 and D_{15} through the period of analysis are highly correlated ($r = 0.99$). The correlation dimension (D_2) is significantly greater than the other multifractal dimensions (i.e.

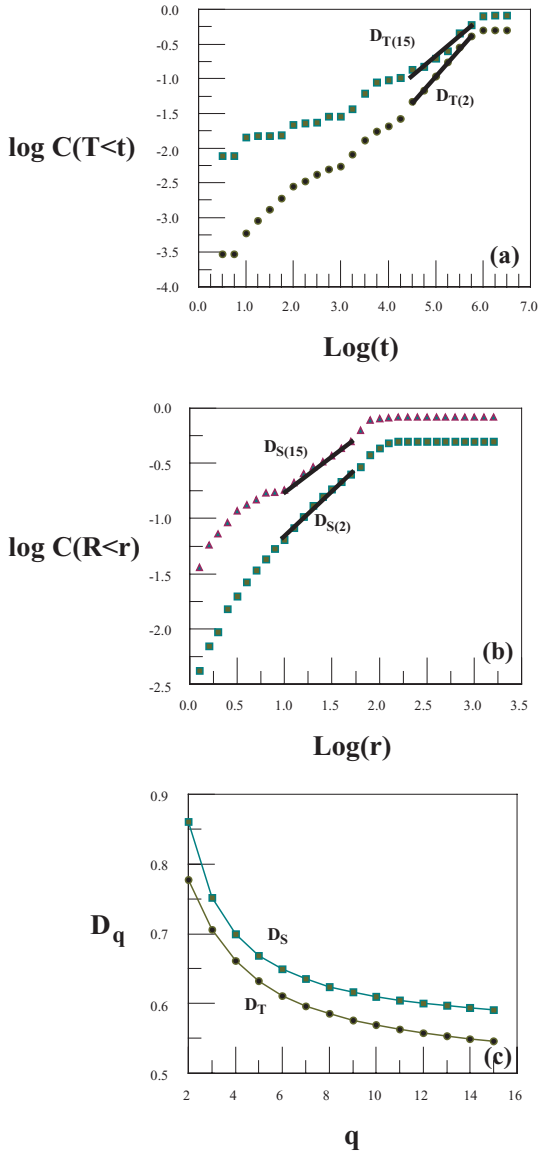

Figure 5. (a) Temporal [logC(t) versus log(t in min)] and (b) spatial [log $C(r)$ versus log(r in km)] fractal plots are presented for multifractal dimensions q equal to 2 and 15. (c) Variations of $D(S)$ and $D(T)$ are shown as a function of q.

q = 3–15) and varies from 0.7 to 1.22 (Fig. 6c). D_{15} (S) varies from 0.44 to 1. These observations suggest, as we would expect, that seismicity is more clustered at local scales defined by D_{15} than at more regional scales defined by D_2. Temporal values of multifractal dimension (Fig. 6d) vary from approximately 0.65–0.85 at regional scale (i.e. $q = 2$) and from approximately 0.3–0.6 at local scale ($q = 15$). Median values of $D_2(T)$ and $D_{15}(T)$ through the period of analysis are less than 1 (0.7 and 0.5, respectively). Values of $D_T < 1$ are indicative of clustering; whereas $D_T > 1$ is associated with more dispersed and randomly distributed hypocentre distributions (Kagan & Jackson 1991).

$D_2(T)$ and $D_2(S)$ converge during the initial 1.5 yr of the analysis window and generally parallel each other throughout the remainder of the observation period (Fig. 8a). Correlation between temporal [$D_2(T)$] and spatial clustering [$D_2(S)$] oscillates from positive to negative (Fig. 8b). There are three periods of positive correlation between $D_2(S)$ and $D_2(T)$ peaking in 1993, mid-1995 and late 1997. Variations in r are evaluated in terms of the probability (p-value) that these correlation coefficients could actually be 0 or have opposite sign. Using a cut-off probability of 0.05, two of these positive correlations can be considered significant: one with p-value of 0.005 (late 1992) and the other with p-value of 0.01 (late 1997). The positive correlation in 1995 is not significant. The variations in D_2 from late 1993 on, are relatively minor, and generally parallel each other (Fig. 8a). Periods of negative correlation (early 1994 and 1996) are not significant. The positive correlations are associated with increasingly clustered seismicity in time and space (1992 to mid-1993) or small decreases in time–space clustering during the later part of the observation period (1996 to mid-1998).

Overall, the general relationship between $D_{15}(S)$ and $D_{15}(T)$ during the observation period is similar to that between $D_2(S)$ and $D_2(T)$ (Fig. 8c). However, the intermediate term correlations between $D_{15}(S)$ and $D_{15}(T)$ differ somewhat from those between $D_2(S)$ and $D_2(T)$ (Fig. 8d). Two periods of significant positive correlation appear in the local ($q = 15$) scale variations. The tail-end of a period of positive correlation is observed in early 1993 and an extended period of positive correlation continues from about mid-1995 till the end of the time-series with mean time of 1997.6. The early positive correlation is associated with a parallel decrease in $D_{15}(S)$ and $D_{15}(T)$, while the extended period of positive correlation is associated generally with parallel increases in $D_{15}(S)$ and $D_{15}(T)$. The time–space variations in D_2 and D_{15} are fairly similar. Both are characterized by periods of increased clustering (drop in D) during the 1992 to mid-1993 time period. Towards the end of the observation period (mid-1998), increases of D associated with increasingly dispersed seismicity are accompanied by a period of anomalously low magnitude seismicity and increased event rate (Figs 6a and b, respectively).

4.1.2 Statistical comparisons

Detailed statistical comparisons of temporal and spatial variations in D (Fig. 8) and variations of b and $D_2(S)$ (Fig. 9) for the 8.5 yr period preceding the Izmit event reveal complex short-term variability. In each comparison, correlation coefficients were computed for consecutive intervals containing eight time steps. The time steps are variable because parameters were computed for windows containing 100 seismic events and the centre of each window was separated from the next by 10 events. The time associated with each point (Figs 8 and 9) is the average time for the data contained in each 8-point window. On average, the correlations are computed at approximately 0.25 yr intervals. While significant overlap in the data from one window to the next ensures similar correlation between consecutive time windows, consistent long-term correlation differences are present. The probability (p) that these correlation coefficients could actually be zero or have opposite sign is also plotted as an indication of the reliability of the correlation coefficient (Figs 8 and 9). A cut-off value of p for significance was set at 0.05 so that p-values $\leq$0.05 are taken as an indication that significant positive and negative correlations are present. As expected, the correlations become insignificant (p-values become greater than 0.05) during phase transitions when the correlation coefficients change from positive to negative or vice versa.

Frequency magnitude plots (Fig. 10) illustrate subtle to significant variation in b-value through time. The plots are referenced to sequentially numbered calculation points labelled in Fig. 9. The frequency magnitude plots include data from the 8 point time

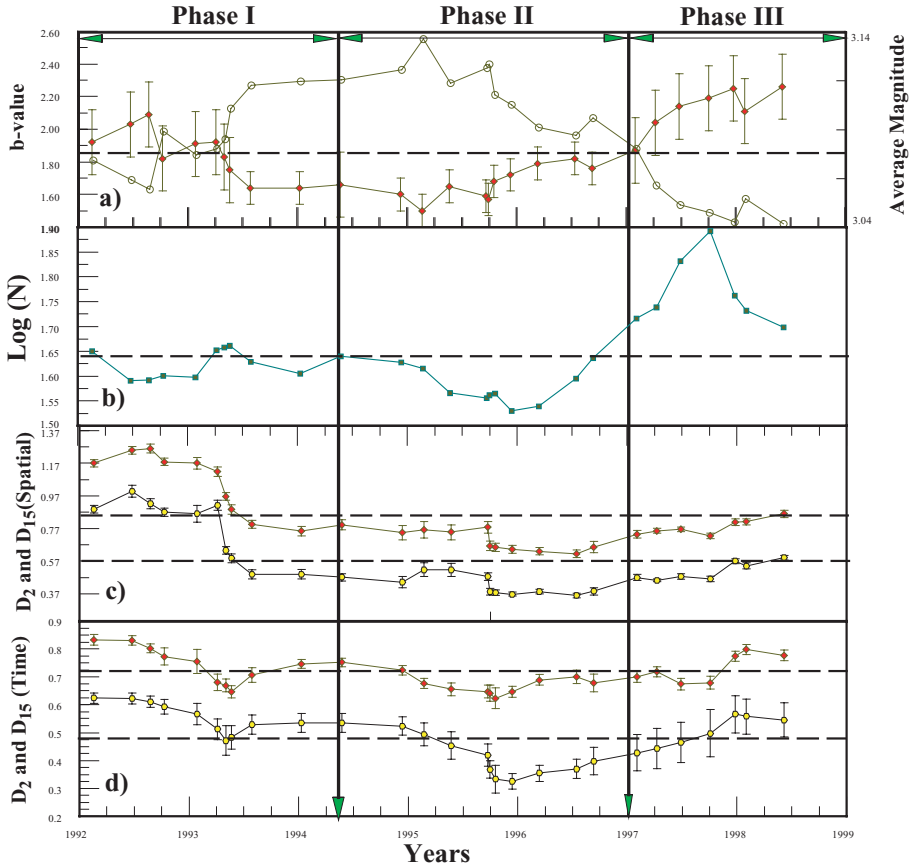

Figure 6. Seismotectonic parameters evaluated in this study are presented together for comparison. (a) *b*-value and average magnitude for moving time windows; (b) Log (N) (where $N = n/T_{\text{obs}}$ and $n = 100$); (c) and (d) Spatial and temporal fractal dimensions D_2 and D_{15} are presented along with their standard errors. The plots are divided into three periods of behaviour: phases I–III.

windows used to compute b at calculation points 5, 13 and 19 (Fig. 9). Each plot is derived from 170 events. These 170 event intervals correspond approximately to 4-yr time intervals (see specific time intervals in Fig. 10). The 95 per cent confidence limits on b are noted in each figure. The shift in *b*-value between phases I and II (calculation points 5 and 13) is only 0.08 and not significantly different. The 0.2 difference in *b*-value between phases II and III (calculation points 13 and 19) is significant at the 95 per cent confidence limit.

4.1.3 Phase changes and variations in strain distribution

The relationship between *b* and $D_2(S)$ (Fig. 6) reveals three phases of significant correlation (p approximately equal to zero) referred to as Phase I, II, and III (see also Fig. 6). Phase I represents a period of positive correlation that extends from late 1992 to mid-1994.4 (Figs 9b and 11). A second period of positive correlation (Phase III) extends from mid-1996 to mid-1998. The interval of time between these two periods is associated primarily with the transition from positive to negative correlation and back again. The intervening period of negative correlation (Phase II) is interpreted to extend approximately from 1994.4 to mid-1996 and includes the transition periods (Figs 9 and 11). As noted earlier, effects on completeness magnitude associated with changes in the seismograph array prior to 1990 have been eliminated by confining our analysis to events recorded in the 1990–1998 time period. Within this context, variations appearing in the data (e.g. Figs 9 and 11) are the result primarily of changes in tectonic stress.

The interrelationships between *b* and $D_2(S)$ that lead to positive and negative correlation are portrayed in Fig. 11. Periods of positive correlation occur in two different ways. The first period of positive correlation (Phase I) is associated with a period during which *b* and $D_2(S)$ decline together (1992 to1994.4, Fig. 11). These changes are associated with clustering of higher magnitude seismicity and suggest that seismic strain release is more concentrated during Phase I. Earthquake magnitude increases to about 3.1 during this phase. A second period of positive correlation between $D_2(S)$ and *b* returns in 1997 (Phase III). This phase is associated with a large increase in *b*-value (see Fig. 3a), a substantial growth in seismicity rate (Fig. 6b) and slight increases in $D_2(S)$. The average magnitude during Phase III drops to approximately 3.04. While these events do not fall in the category of intermediate magnitude earthquakes that Jaume & Sykes (1999) note sometime precede a major earthquake, these variations are significant and precedent. Phase III behaviour is suggestive of the negative feedback process (Henderson & Main 1992) in which there is an absence of interaction between distributed fault segments. The rapid increase of *b* and log (N) suggest that slip is beginning to occur on smaller segments of the Izmit–Sapanca fault. During Phase III, *b* and $D_2(S)$ rise together. Seismicity becomes less clustered, rising approximately from 0.65 to 0.9 (see Figs 9 and 11); however, it remains relatively concentrated with $D_2(S) < 1$. The negative correlation period (Phase II) is associated with an increase in b (dropping magnitude) followed by a decrease in $D_2(S)$

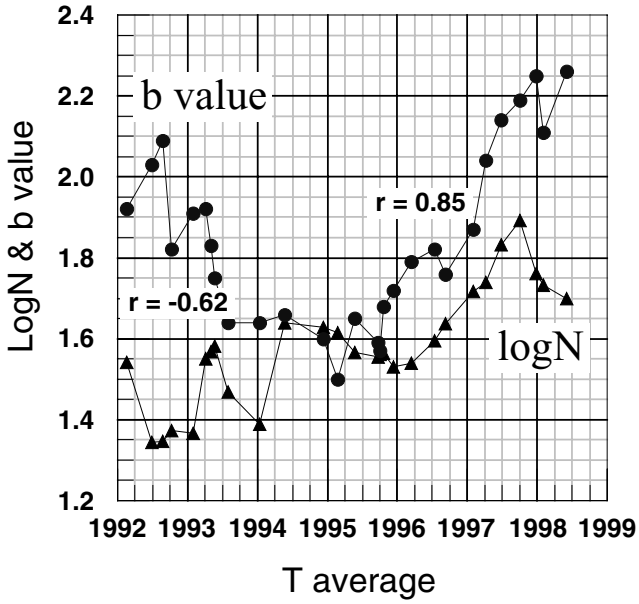

Figure 7. Variations of *b*-value and event rate [log (*N*)] are compared for the 1992 to 1998.5 time period.

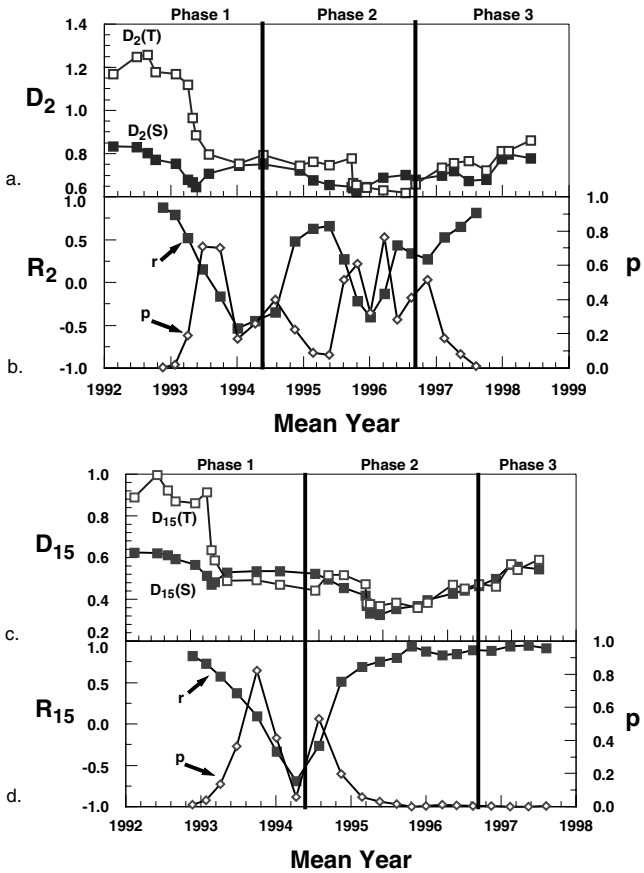

Figure 8. Comparisons of spatial and temporal correlation as a function of time are presented: (a) $D_2(S)$ and $D_2(T)$; (b) Correlation between $D_2(S)$ and $D_2(T)$ and associated *p*-values; (c) $D_{15}(S)$ and $D_{15}(T)$; (d) Correlation between $D_{15}(S)$ and $D_{15}(T)$ and associated *p*-values. Subdivisions corresponding to phases I to III are shown.

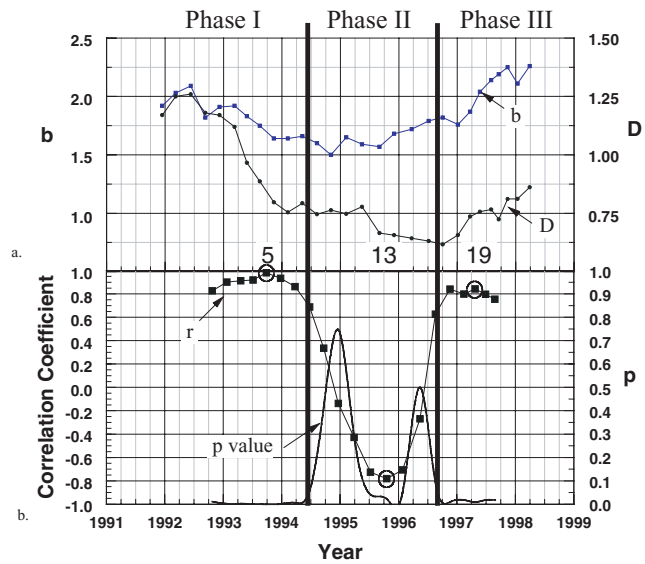

Figure 9. (a) $D_2(T)$ and *b*-value are compared during the 1992 to 1998.5 time interval. (b) The correlation (*r*) between *D*2(*T*) and *b* are followed through time. Variations in *p*-value (probability that the correlation coefficient is significantly different from zero) are also plotted for reference. Phases I through III associated with periods of positive and negative correlation are identified and correlation points 5, 13 and 19 are circled for reference in Fig. 11.

(increased clustering) extending from approximately mid-1994 to mid-1996 (Fig. 11). Overall, these changes suggest that strain release becomes increasingly clustered on smaller fault segments a few years preceding the Izmit event. The pattern of maximum strain distribution along the fault zone also suggests that this is the case (Fig. 1). Maximum strain is less along the central portion of the rupture zone and the magnitude of maximum strain in this region is narrower than to the east and west.

5 DISCUSSION OF OBSERVATIONS

The steady increase in *b*-value in the 2-yr period preceding the Izmit event is similar to that observed prior to rupture of laboratory scale rock fracture experiments (Main *et al.* 1989; Smith 1986; Henderson *et al.* 1994; Lei *et al.* 2000). In their experiments, *b*-value associated with microseismicity in core samples increased to approximately two prior to failure.

Anomalous variations in *b*-value often occur prior to major earthquakes. Fielder (1974) and Smith (1981, 1986) reported intermediate-term increases of *b*-value preceding large earthquakes in New Zealand associated with dip slip fault displacements. Smith (1981) also suggested that this attribute could be characterized by a parameter he called the total precursor time (*T*). Smith computed the precursor time from magnitude using the relationship Log T (days) $= 1.42+0.30\ M$ (see Table 1 of Smith 1981). Using $M_D = 6.8 (M_w = 7.4)$ for the Izmit event yields a precursor time of 7.9 yr. This is considerably longer than the 4–5 yr rise time preceding the Izmit event. Smith's (1981) precursor time is derived for earthquakes associated with thrust faults. Precursor times along strike-slip faults such as the Izmit Sapanca fault may be intrinsically different.

Main & Meredith (1989) note the presence of critically low values of *b*(approximately 0.5) preceding the Western Nagano earthquake

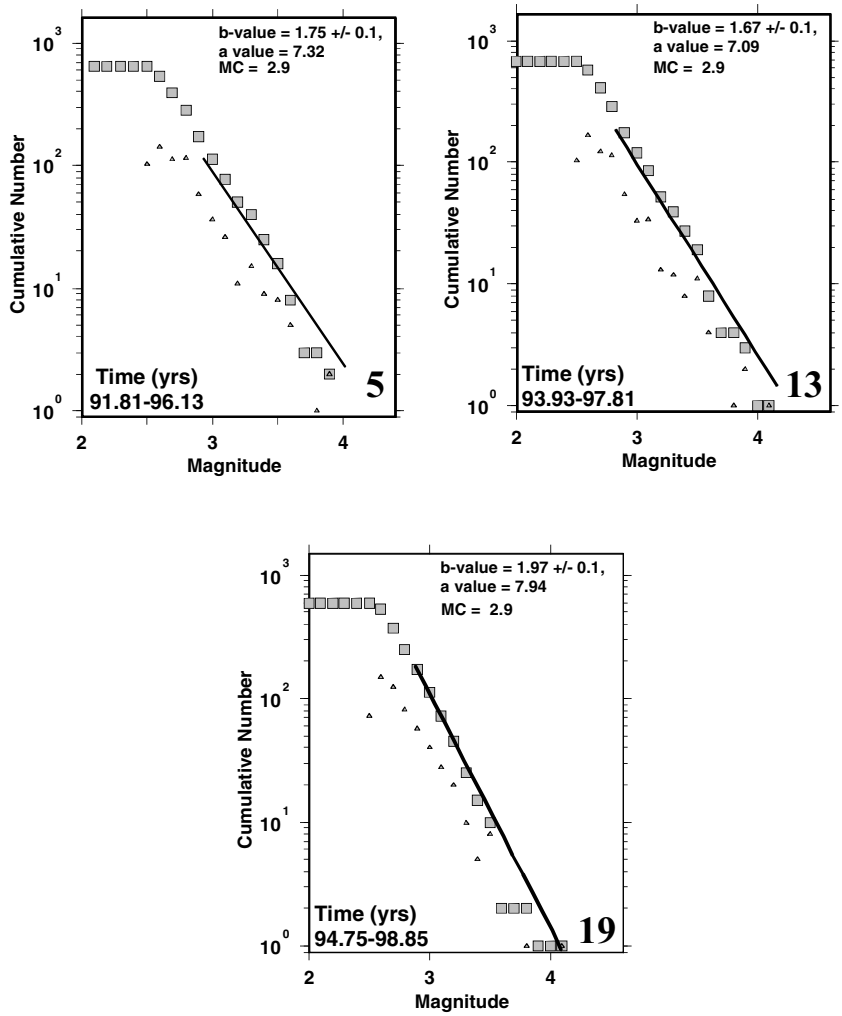

Figure 10. Cumulative (squares) and discrete (triangles) frequency-magnitude statistics are shown for correlation points 5, 13 and 19 located in Fig. 9. The duration of the time window is shown in each frequency magnitude plot.

of 1984. At Nagano, decreasing *b* value was accompanied by periods of seismic quiescence. In their study, laboratory experiments revealed similar decreases in *b*-value prior to rupture. Main & Meredith (1989) indicate, however, that the drop in *b*-value by itself is not sufficient to issue high-level warnings, noting that a similar drop of *b* value was observed in 1983 which gave rise to a false alarm in the Nagano area. Jaume & Sykes (1999) also report decreased *b*-values associated with an increased frequency of intermediate magnitude events (generally $M > 5.0$) preceding large or great earthquakes ($M > 6.5$–7.0). The size of the region associated with these earthquakes scales in proportion to the magnitude of the subsequent main shock suggesting that $D(S)$ would increase during this phase. The analysis of Karakaisis (2003) reveals a long period of decreasing *b*-value from 1981 to 1996 for an area that includes all of western Turkey. Since this region includes a major strike-slip zone, a zone of extension in west-central Turkey, and a zone of compression to the south, it does not isolate and is not representative of behaviour associated with the Izmit fault zone. Analysis presented by Oncel & Wilson (2002) for western Turkey reveal general increases in *b* from 1945 to approximately 1975 that give way to oscillations in *b*-value along the western segment of the Northern Anatolian Fault Zone (see their Fig. 3a). The results obtained in the present study (e.g. Figs 6, 7, and 9) cannot be compared directly to those of Oncel & Wilson (2002) due to the differences in the size of the area investigated, changes in station density and completeness magnitude, and the interval of time over which the analysis was conducted. However, a general comparison does suggest that *b* and *D* have been unstable in the region for approximately 25 yr preceding the Izmit event.

The contrasting observations cited above may be associated with differences in the ability to resolve variations over short time intervals. The observations of Main *et al.* (1989) revealed that *b*-value preceding the 1984 Western Nagano event increased from a low of about 0.6 (approximately 2 yr prior to the event) to 1.2 about 4 months prior to the event. The *b*-value then dropped rapidly from 1.2 to 0.6 during the 4 month period immediately preceding the event. The earlier rise in *b*-value was suggested by Main *et al.* (1989) to result from diffusion of pore fluids into the fault zone and reduced pore pressure (see Fig. 3 of Main *et al.* 1989). The periods during which *b*-value dropped were associated with pore pressure increase and seismic quiescence. If the numbers of events exceeding the threshold magnitude are not sufficient to allow statistically significant estimates of *b*-value over such short time frames, the drop in *b*-value may not be observed. In Vinciguerra's (2002) analysis of seismicity preceding the 1989 eruption of Mt. Etna, a sudden drop in *b*-value was also observed. The abrupt drop of *b*

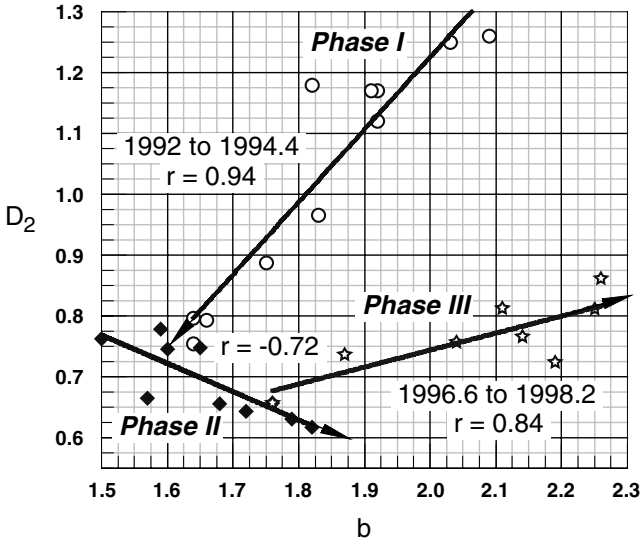

Figure 11. This figure illustrates the three different phases of behaviour observed between b and D_2 (see also Fig. 6). Phases I and III illustrate behaviour during the periods of positive correlation observed in Fig. 6. Phase II illustrates the relationship between *b*-value and D_2 in the intervening period of negative correlation. Arrows on the regression lines indicate the direction of change occurring during each phase.

occurred over a few days ending an approximately 3 month long period of gradually dropping or constant *b*. At the time of eruption *b* dropped to approximately 0.5 similar to that observed by Main & Meredith (1989).

It has been argued that the upper limit of the *b*-value should theoretically not exceed 1.5 (see Olsson 1999). The *b*-value of global seismicity derived from larger moment magnitude events is approximately 1.0 (e.g. Kagan & Jackson 1994). The *b* values observed along the Izmit–Sapanca fault exceed 2.2 for a short time and are generally greater than 1.5. At more local scales *b* varies from 0.5 to 1.6 (e.g. Oncel & Wyss 2001). The *b*-values observed by Main & Meredith (1989) in the 5-yr period preceding the Western Nagano event reached a maximum of only 1.4. Observational data, however, suggest that *b*-values as large 2.2–2.5 may be observed (Smith 1986; Westerhaus *et al.* 2002; Henderson & Main 1992). Similar results are also obtained from experimental seismology (Lei *et al.* 2000). The discrepancies between theory and observation may be associated with distinctions between micro and macroseismicity (Kagan & Jackson 1994). We observed a maximum *b*-value of 2.25, similar to that observed by Henderson & Main (1992) preceding the 1983 Coalinga earthquake near Parkfield ($M = 6.7$). While the increase in *b*-value preceding the Izmit event is not associated with intermediate magnitude seismicity as reported by Jaume & Sykes (1999), for longer time periods the increase in *b* value and event frequency preceding the Izmit event is significant. Our results strongly support the need to establish dense local networks since variations in the frequency of lower magnitude seismicity may serve as important indicators of underlying instability that may precede large events. The larger volume of lower magnitude seismicity also allows seismologists to evaluate seismic behaviour on shorter time frames. Analysis of short-term low magnitude and microseismic activity may yield important insights into the nature of processes that precede and precipitate larger events.

The analysis of D_q reveals an early period (Phase I) where *D* is high and seismicity is dispersed ($D_2 > 1$). *D* (*S* and *T*) are significantly lower during Phases II and III. The end of Phase I is characterized by clustered seismicity,and a drop in magnitude (increased *b*) about 6 yr preceding the Izmit event. About 3 yr prior to the Izmit event (beginning of Phase III), seismicity becomes gradually less clustered, while *b* continues to increase.

6 CONCLUSIONS

We analyzed seismicity in the region surrounding the Izmit Sapanca fault during a 7.4 yr period (1991–1998.4) preceding the 1999 Izmit event ($M_D = 6.8$ or $M_w = 7.4$). The study area lies in northwestern Turkey between 40.5° to 41° north latitude, and 29° and 31° east longitude. Seismic events during this time were subdivided into smaller overlapping time intervals for analysis and comparison.

The correlation between *b* and *D* varied from significantly positive to negative and back again during the analysis period. Oscillations in *b*-value have been reported by others (see Main & Meredith 1989; Henderson & Main 1992; Vinciguerra 2002). The results of this study reveal anomalous behaviour in the intermediate-term seismicity preceding the Izmit event. Phase III seismicity, approximately 1.5–3 yr preceding the event, remained clustered, and was characterized by a rapid rise in *b* from 1.6 to 2.26. Over the long-term (approximately 50 yr), fluctuations in *b*-value reached higher and higher peaks (Fig. 8). In western Turkey, *b*-value rose from 1.6 in 1974 to 2.1 in 1992 and then to 2.26 in 1998. We are missing the details of these variations from 1985 to 1992 and for the 1.5 yr immediately preceding rupture. A similar increase is observed in the yr leading up to the Coalinga earthquake (Henderson & Main 1992). Examination of data presented by Henderson & Main (1992) shows that oscillations in *b*-value reached their highest value about 3 months preceding final rupture. The *b*-value rose to maxima of 1.8 and 1.85 in 1973 and 1976, respectively, before rising to approximately 2.25 prior to the Coalinga event.

We observe positive correlations between *D* and *b* when the *b*-value is high and high negative correlation when the *b*-value is relatively low (Fig. 9). This suggests that in the Izmit area, as the probability of large earthquakes increases (lower *b*-value) there is a corresponding tendency for seismicity to become increasingly clustered. Concentration of maximum GPS strain along the rupture zone appears to be a long-term characteristic of the Izmit–Sapanca fault segment from 1988 to 1998, leading up to final rupture (see Fig. 1). This also corresponds to a time during which *D* remains close to or less than 1 (thus relatively clustered) and during which *b* increases. The final period of anomalous behaviour preceding the Izmit event (Phase III, Figs 9 and 11) is associated with accelerated low magnitude seismicity (increasing *b*-value) during which seismicity becomes more dispersed but remains relatively clustered with ($D < 1$). This behaviour is similar to the negative feedback process described by Henderson & Main (1992) in which strain release becomes increasingly dispersed while event magnitude drops. At Izmit, the results suggest that rupture occurs on faults with smaller and smaller surface area during this phase. Henderson & Main (1992) observe a period of positive feedback in which faults begin to coalesce leading to larger magnitude events. We do not observe this phenomenon; however, we suspect that the period of accelerated seismicity associated with Phase III eventually led to coalescence of fault surfaces and final rupture. We did not see the drop in *b*-value often reported to precede a major event. This drop, if it occurred, appears to have been fairly abrupt in the case of the 1999 Izmit event. Data presented by Henderson *et al.* (1992) for the Coalinga earthquake near Parkfield, California, indicate that this drop can be quite sudden, appearing

only 2–3 months prior to rupture. The frequency of earthquake occurrence may not permit a statistically accurate short-term estimate of the *b*-value. In cases where the number of observed events preceding main rupture is too low to resolve the drop in *b*-value, cycles of accelerated low magnitude seismic activity in which *b* becomes anomalously high (>2) may serve as an early warning of an impending large magnitude rupture. Analysis of microseismic data provided by increasingly dense seismic networks will shorten the period of analysis needed to identify statistically significant trends in seismic behaviour.

ACKNOWLEDGMENTS

We appreciate the comments of Dr. Ian Main and Steven Ward. Appreciation is also extended to Dr Xinglin Lei who provided use of his software to determine multifractal dimensions. Also, we appreciate Dr Awata from GSJ, who provided us his data on measured slip. The comments of anonymous reviewers and the journal editor were very helpful and much appreciated.

REFERENCES

Aki, K., 1965. Maximum likelihood estimate of b in the formula logN=a-bM and its confidence limits, *Bulletin Earthquake Research Institute of Tokyo University,* **43,** 237–239.

Ambraseys, N., 2002. 'The seismic activity of the Marmara Sea region over the last 2000 years', *Bull. seism. Soc. Am.,* **92**(1), 1–18.

Awata, Y. *et al.*, 2003. Outline of the surface rupture of 1999 Izmit earthquake, in *Surface rupture associated with the August 17, 1999 Izmit earthquake*, pp. 41–50, MTA, Ankara.

Baker, G.L. & Gollub, J.P., 1990. *Chaotic Dynamics: An Introduction*, Cambridge University Press, New York, 182p.

Castellaro, S., Mulargia, F. & Kagan, Y.Y., 2006. Regression problems for magnitudes, *Geophys. J. Int.,* **165**(3), 913–930.

Evans, R., Asudeh, I., Crampin, S. & Ucer, B., 1982. Microtectonics in the Marmara Sea Region, *Geophys. J. R. astr. Soc.,* **69**(1), 284–284.

Evans, R., Asudeh, I., Crampin, S. & Ucer, S.B., 1985. Tectonics of the Marmara Sea Region of Turkey - New Evidence from Micro-Earthquake Fault Plane Solutions, *Geophys. J. R. astr. Soc.,* **83**(1), 47–60.

Fielder, G., 1974, Local b-values to seismicity, *Tectonophysics,* **23,** 277–282.

Godano, C. & Caruso, V., 1995. Multifractal Analysis of Earthquake Catalogs, *Geophys. J. Int.,* **121**(2), 385–392.

Grassberger, P. & Procaccia, I., 1983. Measuring the strangeness of strange attractors, *Physica,* **9D,** 189–208.

Gutenberg, B. & Richter, C.F., 1954. *Seismicity of the Earth and Associated Phenomena*, Princenton University Press, Princeton.

Henderson, J. & Main, I., 1992. A Simple Fracture-Mechanical Model for the Evolution of Seismicity, *Geophys. Res. Lett.,* **19**(4), 365–368.

Henderson, J., Main, I., Meredith, P.G. & Sammonds, P.R., 1992. The evolution of seismicity at Parkfield:observation, experiment and a fracture-mechanical interpretation, *J. Struct. Geol.,* **14,** 905–913.

Henderson, J., Main, I., Maclean, C. & Norman, M.G., 1994. A Fracture-Mechanical Cellular Automation Model of Seismicity, 142, *Pure. appl. Geophys.,* **19**(4), 545–565.

Ito, A. *et al.*, 2002. Aftershock activity of the 1999 Izmit, Turkey, earthquake revealed from microearthquake observations, *Bull. seism. Soc. Am.,* **92**(1), 418–427.

Jaume, S.C. & Sykes, L.R., 1999. Evolving towards a critical point: a review of accelerating seismic moment/energy release prior to large and great earthquakes, *Pure appl. Geophys.,* **155,** 279–305.

Kahle, H.G., Cocard, M., Peter, Y., Geiger, A., Reilinger, R., Barka, A. & Veis, G., 2000. GPS-derived strain rate field within the boundary zones of the Eurasian, African, and Arabian Plates, *J. Geophys. Res.-Solid Earth,* **105**(B10), 23 353–23 370.

Kagan, Y.Y. & Jackson, D.D., 1991. Long-term earthquake clustering, *Geophys. J. Int.,* **104,** 117–133.

Kagan, Y.Y. & Jackson, D.D., 1994. Long-term probabilistic forecasting of earthquakes, *J. Geophys. Res. Earth,* **99**(B7), 13 685–13 700.

Karakaisis, G.F., 2003. Accelerating seismic crustal deformation before the Izmit earthquake (NW Turkey) large mainshock of 1999 August 17 and the evolution of its aftershock sequence, *Geophys. J. Int.,* **153,** 103–110.

Kostrov, B.V., 1974. Seismic moment and energy of earthquakes and seismic flow of rock, *Izvestiya-Phys. Solid Earth,* **1,** 23–40.

Lei, X.L. & Kusunose, K., 1999. Fractal structure and characteristic scale in the distributions of earthquake epicentres, active faults and rivers in Japan, *Geophys. J. Int.,* **139**(3), 754–762.

Lei, X.L., Kusunose, K., Rao, M.V.M.S., Nishizawa, O. & Satoh, T., 2000. Quasi-static fault growth and cracking in homogeneous brittle rock under triaxial compression using acoustic emission monitoring, *J. Geophys. Res. Soild Earth,* **105**(B3), 6127–6139.

Main, I., 1996. Statistical physics, seismogenesis, and seismic hazard, *Rev. Geophys.,* **34**(4), 433–462.

Main, I. & Meredith, P.G., 1989. Classification of earthquake precursors from a fracture mechanics model, *Tectonophysics,* **167,** 273–283.

Main, I.G., Meredith, P.G. & Jones, C., 1989. A reinterpretation of the precursory seismic b-value anomaly from fracture mechanics, *Geophys. J. Int.,* **96,** 131–138.

Nakaya, S. & Hashimoto, T., 2002. Temporal variation of multifractal properties of seismicity in the region affected by the mainshock of the October 6, 2000 Western Tottori Prefecture, Japan, earthquake (M = 7.3), *Geophys. Res. Lett.,* **29**(10), art. no.–1495.

Olsson, R., 1999. An estimation of the maximum b-value in the Gutenberg-Richter relation, *Geodynamics,* **27,** 547–552.

Öncel, A.O. & Alptekin, Ö., 1999. Microseismicity of Marmara Sea and Seismic Hazard, pp. 40, Research Foundation of Istanbul University.

Öncel, A.O., Alptekin, Ö. & Main, I., 1995. Temporal variations of the fractal properties of seismicity in the western part of the northAnatolian fault zone:possible artifacts due to improvements in station coverage, *Nonlinear proc. Geophys.,* **2,** 147–157.

Oncel, A.O., Main, I., Alptekin, O. & Cowie, P., 1996. Temporal variations in the fractal properties of seismicity in the North Anatolian Fault Zone between 31 degrees E and 41 degrees E, *Pure appl. Geophys.,* **147**(1), 147–159.

Oncel, A.O. & Wilson, T.H., 2002. Space-time correlations of seismotectonic parameters: Examples from Japan and from Turkey preceding the Izmit earthquake, *Bull. seism. Soc. Am.,* **92**(1), 339–349.

Oncel, A.O. & Wyss, M., 2000. Mapping the major asperities by minima of local recurrence time before the 1999 M7.4 Izmit earthquake, in *The Izmit and Duzce Earthquakes: preliminary results*, pp. 1–14, Istanbul Technical University, Istanbul.

Oncel, A.O. & Wyss, M., 2001. The major asperities of the 1999 M-w = 7.4 Izmit earthquake defined by the microseismicity of the two decades before it, *Geophys. J. Int.,* **143**(3), 501–506.

Oncel, A.O. & Wilson, T., 2004. Correlation of seismotectonic variables and GPS strain measurements in western Turkey, *J. Geophys. Res. Solid Earth,* **109,** B11306, 13 pages.

Oncel, A.O. & Wilson, T.H., 2006. 'Evaluation of earthquake potential along the Northern Anatolian Fault Zone in the Marmara Sea using comparisons of GPS strain and seismotectonic parameters.' *Tectonophysics,* **418,** 205–218.

Scholz, C.H., 2002. Earthquakes and Faulting, Cambridge University Press, Cambridge.

Shaw, B.E., 1993. Generalized Omori law for aftershocks and foreshocks from a simple dynamics, *Geophys. Res. Lett.,* **20,** 907–910.

Shaw, B.E. & Carlson, T.M., 1992. 'Patterns of seismic activity preceeding large earthquakes', *Geophys. J. R. astr. Soc.,* **97,** 479–488.

Shah, K.R. & Labuz, F.J., 1995. Damage mechanisms in stressed rock from acoustic emission, *J. Geophys. Res.-Solid Earth,* **100,** 15 527–15 539.

Smalley, R.F. Jr., Chatelian, J.L., Turcotte, D.L. & Prevot, A., 1987. A fractal approach to the clustering of earthquakes: applications to the seismicity of New Hebrides, *Bull. seism. Soc. Am.,* **77,** 1368–1381.

Smith, D.W., 1981. The b-value as an earthquake precursor, *Nature,* **289,** 136–139.

Smith, D.W., 1986. Evidence for precursory changes in the frequency-magnitude b-value, *Geophys. J. R. astr. Soc.,* **86,** 815–838.

Steacy, S. & McClusky, S., 1999. Heterogeneity and the earthquake magnitude-frequency distribution, *Geophys. Res. Lett.,* **26**(7), 899–902.

Sunmonu, L.A., Dimri, V.P., Prakash, M.R. & Bansal, A.R., 2001. Multi-fractal approach to the time series of $M >= 7.0$ earthquake in Himalayan region and its vicinity during 1895–1995, *J. Geol. Soc. India,* **58**(2), 163–169.

Toksoz, M.N., Shakal, A.F. & Michael, A.J., 1979. Space-time migration of earthquakes along the North Anatolian fault zones and seismic gaps, *Pure appl. Geophys.,* **117,** 1258–1270.

Ucer, S.B., Crampin, S., Evans, R., Miller, A. & Kafadar, N., 1985. The Marnet Radiolinked Seismometer Network Spanning the Marmara Sea and the Seismicity of Western Turkey, *Geophys. J. R. astr. Soc.,* **83**(1), 17–30.

Vinciguerra, S., 2002. Damage mechanics preceding the September-October 1989 flank eruption at Mount Etna volcano inferred by seismic scaling exponents, *J. Volc. Geother. Res.,* **113,** 391–397.

Ward, S., 1994. A multidisciplinary approach to seismic hazard in southern California, *Bull. Seism. Soc. Am.,* **84**(5), 1293–1309.

Westerhaus, M., Wyss, M., Yilmaz, R. & Zschau, J., 2002. Correlating variations of b-values and crustal deformations during the 1990s may have pinpointed the rupture initiation of the $M_w = 7.4$ Izmit earthquake of 1999 August 17, *Geophys. J. Int.,* **148**(1), 139–152.

Wiemer, S. & Wyss, M., 2000. 'Minimum magnitude of completeness in earthquake catalogues: Examples from Alaska, the western United States, and Japan.' *Bull. Seism. Soc. Am.,* **90**(4), 859–869.

Wiemer, S., 2001. 'A software package to analyze seismicity: ZMAP.' *Seism. Res. Lett.,* **72,** 373–382.